PNAS RESEARCH ARTICLE | MEDICAL SCIENCES

IER3IP1 is critical for maintaining glucose homeostasis through regulating the endoplasmic reticulum function and survival of β cells

Jing Yang[a,1], Jinyang Zhen[a,1], Wenli Feng[a,1], Zhenqian Fan[b], Li Ding[a], Xiaoyun Yang[a], Yumeng Huang[a], Hua Shu[a], Jing Xie[a], Xin Li[a], Jingting Qiao[a], Yuxin Fan[a], Jinhong Sun[a], Na Li[a], Tengli Liu[c,d], Shusen Wang[c,d,e], Xiaona Zhang[a,2], Peter Arvan[f,2], and Ming Liu[a,2]

Edited by Domenico Accili, Columbia University; received March 13, 2022; accepted October 6, 2022 by Editorial Board Member Barbara B. Kahn

Recessive mutations in IER3IP1 (immediate early response 3 interacting protein 1) cause a syndrome of microcephaly, epilepsy, and permanent neonatal diabetes (MEDS). IER3IP1 encodes an endoplasmic reticulum (ER) membrane protein, which is crucial for brain development; however, the role of IER3IP1 in β cells remains unknown. We have generated two mouse models with either constitutive or inducible IER3IP1 deletion in β cells, named IER3IP1-βKO and IER3IP1-iβKO, respectively. We found that IER3IP1-βKO causes severe early-onset, insulin-deficient diabetes. Functional studies revealed a markedly dilated β-cell ER along with increased proinsulin misfolding and elevated expression of the ER chaperones, including PDI, ERO1, BiP, and P58IPK. Islet transcriptome analysis confirmed by qRT-PCR revealed decreased expression of genes associated with β-cell maturation, cell cycle, and antiapoptotic genes, accompanied by increased expression of antiproliferation genes. Indeed, multiple independent approaches further demonstrated that IER3IP1-βKO impaired β-cell maturation and proliferation, along with increased condensation of β-cell nuclear chromatin. Inducible β-cell IER3IP1 deletion in adult (8-wk-old) mice induced a similar diabetic phenotype, suggesting that IER3IP1 is also critical for function and survival even after β-cell early development. Importantly, IER3IP1 was decreased in β cells of patients with type 2 diabetes (T2D), suggesting an association of IER3IP1 deficiency with β-cell dysfunction in the more-common form of diabetes. These data not only uncover a critical role of IER3IP1 in β cells but also provide insight into molecular basis of diabetes caused by IER3IP1 mutations.

diabetes | IER3IP1 | ER stress | β cell survival | β cell proliferation

Significance

IER3IP1 mutations cause a syndrome of microcephaly, epilepsy, and permanent neonatal diabetes (MEDS). Here, we demonstrate that IER3IP1 is highly expressed in pancreatic β cells. Constitutive or inducible deletion of IER3IP1 in β cells impairs normal function of endoplasmic reticulum (ER), inducing ER stress and proinsulin misfolding, causing an impairment of β cell maturation and proliferation along with an increase of apoptosis, and leading to insulin-deficient diabetes that can be observed either in neonatal stage (constitutive deletion) or in adulthood (inducible deletion at 8 wk of age). Importantly, the expression of IER3IP1 is markedly decreased in patients with type 2 diabetes, suggesting an important association of IER3IP1 deficiency and β cell dysfunction in the more-common form of diabetes.

Monogenic diabetes mellitus (MDM) caused by single gene mutations accounts for 1–5% of all forms of diabetes (1). To date, mutations in more than 30 distinct genes have been reported to cause MDM (2–4) with impaired β cell function, maturation, and survival (and less commonly, insulin action). Diabetes phenotypes of MDM can range from severe neonatal-onset, insulin-deficient diabetes to childhood or adulthood onset diabetes (MODY [maturity-onset diabetes of the young]). Although the onset and severity of diabetes is largely determined by the mutant alleles that disrupt normal function of affected gene products, environmental factors may also contribute to clinical presentation (5, 6). Single-nucleotide polymorphisms contained within at least half of the listed MDM genes have been associated with risk of type 1 diabetes and/or type 2 diabetes (T2D) (7), suggesting important contributions of MDM genes to more-common forms of diabetes. One such example comes from *INS* gene mutations, which collectively represent the second-most-common genetic cause of permanent neonatal diabetes. Among 70 *INS* gene mutations associated with diabetes, the majority impair proinsulin oxidative folding with defective export from the endoplasmic reticulum (ER) (8–10) while also interacting (and impairing trafficking) of the coexpressed wild-type *INS* gene product, thereby decreasing insulin production (11–13). Proinsulin misfolding with defective formation and storage of mature insulin may also contribute to the development and progression of T2D (14–16).

In addition to MDM, there are 69 genetic syndromes associated with diabetes, of which more than 40% have diabetes as a main clinical presentation (17). MEDS (microcephaly, epilepsy, and diabetes syndrome) is one such syndrome, caused by monogenic mutations in IER3IP1 (immediate early response 3 interacting protein 1) (18–20). The disease is inherited in an autosomal recessive fashion. To date, only nine cases have been reported (21). All described patients have developed similar clinical features, including infantile epileptic encephalopathy, microcephaly, and permanent neonatal diabetes, and all reported patients died before the age of eight (18, 21, 22).

Author contributions: M.L. designed research; J.Y., J.Z., W.F., Z.F., L.D., X.Y., Y.H., H.S., J.X., X.L., J.Q., Y.F., J.S., N.L., T.L., and X.Z. performed research; J.Y., J.Z., W.F., Z.F., L.D., X.Y., Y.H., H.S., J.X., X.L., J.Q., Y.F., J.S., N.L., T.L., S.W., X.Z., and M.L. analyzed data; and J.Y., J.Z., P.A., and M.L. wrote the paper.

The authors declare no competing interest.

This article is a PNAS Direct Submission. D.A. is a guest editor invited by the Editorial Board.

[1]J.Y., J.Z., and W.F. contributed equally to this work.

[2]To whom correspondence may be addressed. Email: zhangxiaona@tmu.edu.cn, parvan@umich.edu, or mingliu@tmu.edu.cn.

This article contains supporting information online at http://www.pnas.org/lookup/suppl/doi:10.1073/pnas.2204443119/-/DCSupplemental.

Published November 2, 2022.

IER3IP1 is an ER membrane protein highly expressed in brain and pancreatic β cells (20, 23); however, its function remains to be fully characterized. One study shows that YOS1P (a yeast IER3IP1 homolog) plays an important role in mediating secretory protein transit between the ER and Golgi complex (24). This appears to be consistent with a recent report revealing that IER3IP1 regulates ER function and extracellular matrix protein secretion crucial for brain development and integrity (25). Indeed, postmortem analysis of patients with MEDS has shown a reduced No. of neurons in the brain cortex along with increased neuronal apoptosis (20). Additionally, postmortem analysis of the pancreas reveals that MEDS patients have a markedly decreased No. of insulin-producing β cells. The underlying mechanism remains to be determined, although one study using the Min6 pancreatic β cell line suggests that IER3IP1 may be involved in the regulation of cell death and proliferation (26).

In this study, we have generated two mouse models with either constitutive or inducible deletion of IER3IP1 in β cells, named IER3IP1-βKO and IER3IP1-iβKO, respectively. IER3IP1-βKO resulted in mild elevated blood glucose at the first day after birth. We find that IER3IP1-βKO causes a dilated β cell ER, accompanied by increased proinsulin misfolding and upregulation of ER chaperones, suggesting that IER3IP1-βKO induces ER stress despite only a modest unfolded protein response (UPR). In addition, islets from IER3IP1-βKO mice exhibit upregulation of genes that impair cell proliferation and downregulation of genes that would normally promote β cell maturation, cell cycle, and survival. With several independent approaches, we demonstrate that IER3IP1 deficiency impairs β-cell maturation and proliferation while favoring chromatin condensation consistent with pyknotic nuclei. Furthermore, inducible IER3IP1 deletion in β cells at 8 wk of age using IER3IP1-iβKO mice also decreased insulin content and caused insulin-deficient diabetes, demonstrating that IER3IP1 remains important for β cells in adulthood. Importantly, we found that the expression of IER3IP1 is decreased in islet β cells of patients with T2D, suggesting that there may be an association of IER3IP1 deficiency with β-cell dysfunction in T2D. These data not only uncover a critical role of IER3IP1 in β-cell function and survival but also provide insight into mechanisms underlying diabetes caused by loss-of-function mutations of IER3IP1.

Methods

Mice. IER3IP1 floxed mice were generated though homologous recombination by genomic insertion of two loxP sites flanking the exon1 of IER3IP1. Pancreatic β cell–specific IER3IP1 knockout mice (IER3IP1-βKO) were generated by crossbreeding of IER3IP1 floxed mice with Rat *Ins2* promoter-driven Cre (RIP-Cre) mice (purchased from The Jackson Laboratory, cat No. 003573). The mice with inducible deletion of IER3IP1 specific in β cells (IER3IP1-iβKO) were generated by crossbreeding of IER3IP1 floxed mice with mouse *Ins1* promoter-driven Cre mice (purchased from The Jackson Laboratory, stock No. 024709). The primers for genotyping of the above mice were shown in *SI Appendix*, Table S1. To activate Cre recombinase, 8-wk-old male mice were treated with tamoxifen (Sigma-Aldrich, CAS No. 10540-29-1) 75 mg/kg body weight via intraperitoneal injection once a day for 5 consecutive days. All mice were housed in a 12 h light/dark cycle in a temperature (22–25 °C) and humidity (55 ± 5%) control room. All mice used in this study were on a C57BL/6J background. Weekly monitor of body weight and blood glucose were performed at the same time of the day for consistency.

Massive Parallel Sequencing of RNA (RNA-Seq) and Analysis. The islets transcriptome analysis was conducted by OE Biotech Co., Ltd. (Shanghai, China). Total RNA extraction, RNA integrity evaluation, libraries construction, and sequencing were performed according to the manufacturer's standard protocol. The differential expressed genes were identified using the absolute value of log2 (ratio) ≥ 1 as the threshold. Gene Ontology (GO) analysis and pathway enrichment studies were performed by WebGestalt, and pathway visualization was conducted by Graph-Pad Prism 8. Additional detailed materials and methods are provided in *SI Appendix, Materials and Methods*.

Study Approval. All animal experiments followed the protocols approved by the Internal Animal Welfare Committee at Tianjin Medical University. Human pancreas tissue was obtained between Jan 2016 and Aug 2020 from nondiabetic and T2D organ donors after informed consent was obtained. The study was approved by the Tianjin First Central Hospital clinical research ethics committee (No. 2020N249KY).

Results

IER3IP1 Is Decreased in β Cells of Patients with T2D, and β Cell–Specific IER3IP1 Knockout Causes Insulin-Deficient Diabetes. By immunofluorescence, we observed that IER3IP1 was highly expressed in islet β cells (but not α cells or δ cells) in both rodent and human pancreas (Fig. 1 *A* and *B*). Importantly, IER3IP1 was markedly decreased in β cells without notable change of expression in α cells in patients with T2D, suggesting an association of IER3IP1 deficiency with β-cell dysfunction in T2D (Fig. 1*C* and *SI Appendix*, Fig. S2*A*). Since the most important characteristic physiological feature of β cells is to synthesize and secrete insulin upon glucose stimulation, we asked whether the expression of IER3IP1 is regulated by glucose in isolated mouse islets treated with low (2.8 mM) and high (16.7 mM) glucose. As expected, high glucose exposure upregulated *INS* mRNA expression (*SI Appendix*, Fig. S2*B*) as well as proinsulin protein level (*SI Appendix*, Fig. S2*C*). However, high glucose exposure did not upregulate IER3IP1 mRNA (*SI Appendix*, Fig. S2*B*) or protein (*SI Appendix*, Fig. S2 *C* and *D*). To further explore the function of IER3IP1 in β cells, we generated a mouse model with β cell–specific IER3IP1 deletion (IER3IP1-βKO) using homologous recombination mediated by RIP-Cre (*SI Appendix*, Fig. S3). A significant decrease of IER3IP1 in the islets was confirmed both by immunohistochemistry (Fig. 1*D*) and western blot (Fig. 1*E*). IER3IP1-βKO resulted in a modest increase of blood glucose and a trend of decreased body weight during the first 14 d of life (Fig. 1 *F* and *G*). Insulin-deficient diabetes became more severe at 3 wk of age in both male and female mice (Fig. 1 *H* and *I*). Over an observation period of 16 wk, hyperglycemia in IER3IP1-βKO mice progressively worsened (Fig. 1*J*) along with impaired body weight gain starting from 11 wk of age in male mice and 3 wk of age in female mice (Fig. 1*K*). Although IER3IP1 mRNA was decreased in heterozygous mice, no significant changes in IER3IP1 protein level were observed (*SI Appendix*, Fig. S4 *A* and *B*). In addition, no differences in glucose tolerance, blood glucose, and body weight were observed between control mice and IER3IP1 heterozygous mice (*SI Appendix*, Fig. S4 *C–H*), indicating that one allele of IER3IP1 is sufficient to maintain normal β-cell function. Taken together, these data demonstrate that IER3IP1 is highly expressed in pancreatic β cells and is required for maintenance of glucose homeostasis.

IER3IP1-βKO Knockout Leads to Decreased Insulin Content and Absolute Amount of Secreted Insulin; However, Glucose Stimulation of Proinsulin Synthesis and Insulin Release Are Preserved. To understand the cause of the insulin-deficient diabetes in IER3IP1-βKO mice, we performed immunostaining and western blotting and observed a significant reduction of proinsulin and insulin content in IER3IP1-βKO islets (Fig. 2 *A–C*). When incubating isolated islets with low (2.8 mM) and high

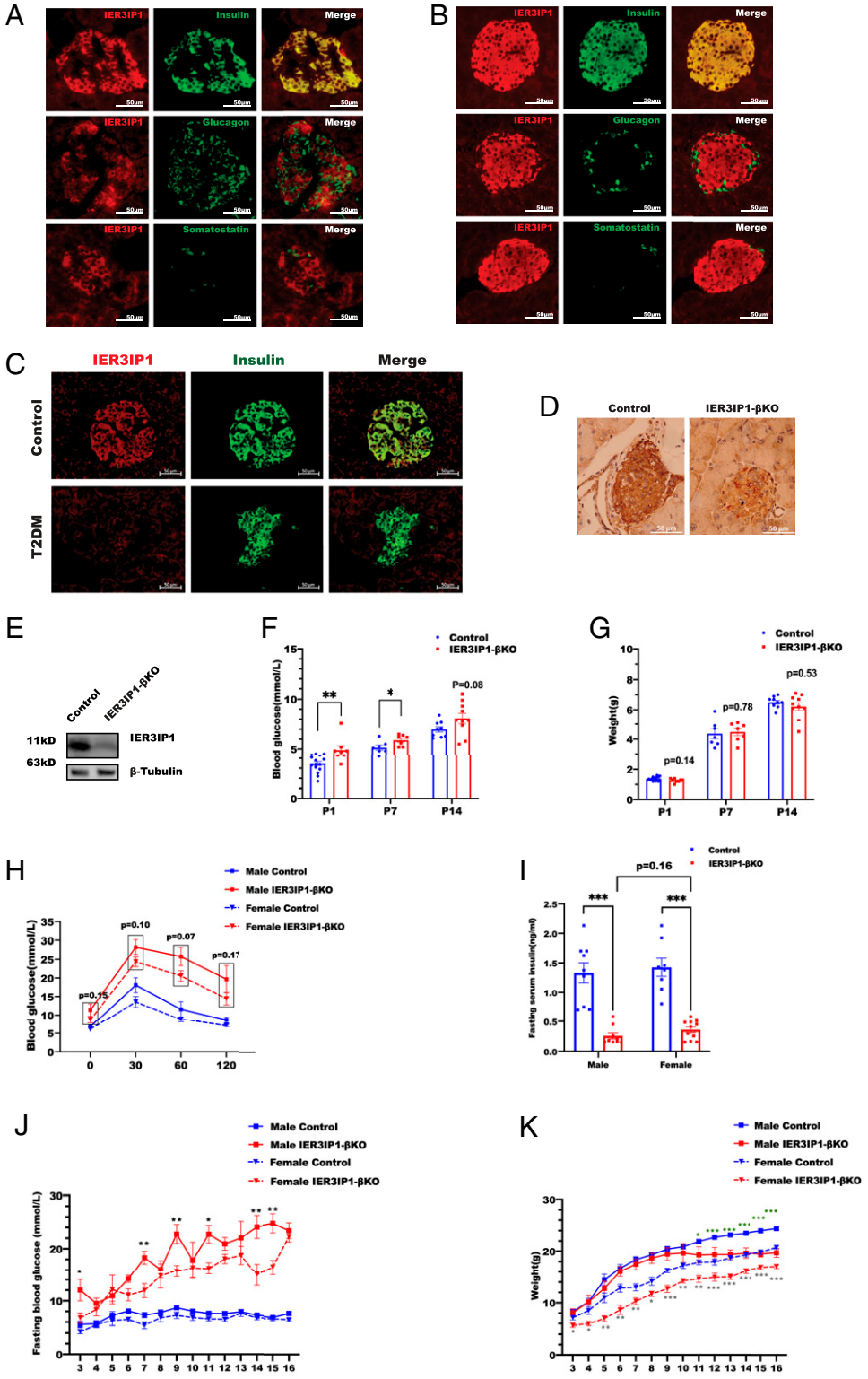

Fig. 1. IER3IP1 is highly expressed in β cells, and IER3IP1-βKO mice develop early-onset, insulin-deficient diabetes. (*A* and *B*) The expression of IER3IP1 in (*A*) human and (*B*) mouse pancreases was detected via the immunostaining with anti-IER3IP1 (red) with anti-insulin (green), antiglucagon (green), or antisomatostatin (green). (*C*) The expression of IER3IP1 in pancreases of donors with T2D were detected via the immunostaining with anti-IER3IP1 (red) and anti-insulin (green). (*D*) Immunohistochemistry staining was performed to detect the expression of IER3IP1 in pancreases of 3-wk-old IER3IP1-βKO mice or flox$^{+/+}$ control mice. (*E*) IER3IP1 protein expression from 3-wk-old flox$^{+/+}$ control mice or IER3IP1-βKO mice was examined by western blotting using anti-IER3IP1. (*F*) Blood glucose (BG) of 1-, 7-, and 14-d-old flox$^{+/+}$ control mice or IER3IP1-βKO mice (control n = 7–15, βKO n = 7–10). *P < 0.05 and **P < 0.01. (*G*) Body weight (BW) of same group mice as *F*. (*H*) Oral glucose tolerance tests were performed in 3-wk-old male (control n = 7, βKO n = 7) and female mice (control n = 10, βKO n = 10). The levels of BG are all higher in both IER3IP1-βKO male and female mice than that of the control mice. However, no statistical differences were observed between male and female IER3IP1-βKO mice. (*I*) Fasting serum insulin levels of 3-wk-old male (control n = 8, βKO n = 9) and female (control n = 8, βKO n = 11) mice were measured using insulin enzyme-linked immunosorbent assay (ELISA). ***P < 0.001. (*J*) Fasting blood glucose of male (control n = 10, βKO n = 5) and female (control n = 10, βKO n = 7) mice was monitored weekly till 16 wk. *P < 0.05 and **P < 0.01, respectively, comparing male and female IER3IP1-βKO mice. (*K*) BWs from same group of *J* were monitored. Asterisks with green color indicate statistical differences between male IER3IP1-βKO and control mice. Asterisks with gray indicate statistical differences between female IER3IP1-βKO and control mice. All values shown in this figure are mean ± SEM. *P < 0.05, **P < 0.01 and ***P < 0.001.

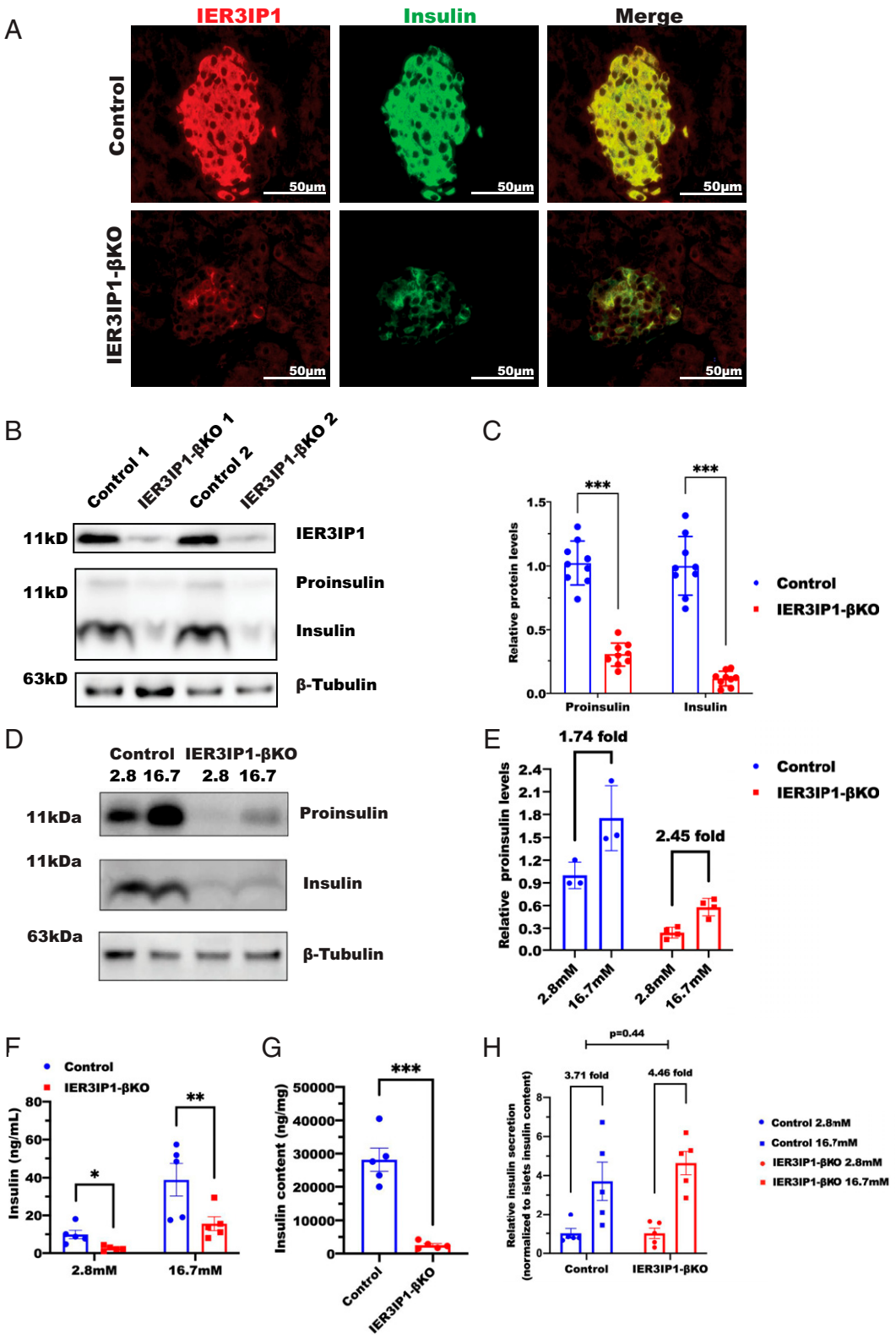

Fig. 2. IER3IP1-βKO leads to decreased insulin content and absolute amount of secreted insulin, however glucose stimulated proinsulin synthesis and GSIS are preserved. (*A*) Representative immunofluorescence images of anti-IER3IP1 (red) and anti-insulin (green) in pancreatic sections from 3-wk-old flox$^{+/+}$ control and IER3IP1-βKO mice. (*B*) Islets isolated from 3-wk-old control and IER3IP1-βKO mice were directly lysated. Western blots were performed to detect proinsulin and insulin, and β-tubulin was used as a loading control. (*C*) Quantification of protein levels of proinsulin and insulin in *B* ($n = 9$). ***$P < 0.001$. (*D*) Islets isolated from 3-wk-old flox$^{+/+}$ control and IER3IP1-βKO mice were incubated with media containing either 2.8 mM or 16.7 mM glucose for 5 h before lysated for western blotting. (*E*) Quantification of fold increases of proinsulin shown in *D* (control $n = 3$, βKO $n = 4$). (*F*) GSIS was performed, and insulin levels were measured in isolated islets from flox$^{+/+}$ control and IER3IP1-βKO mice. (*G*) Insulin content in the islets of *F* were measured using insulin ELISA. (*H*) Secreted insulin was normalized to insulin content of the islets. All experiment shown in *F–H* were performed using islets from 3-wk-old mice ($n = 5$ in each group). Values were shown as mean ± SEM. *$P < 0.05$, **$P < 0.01$, and ***$P < 0.001$.

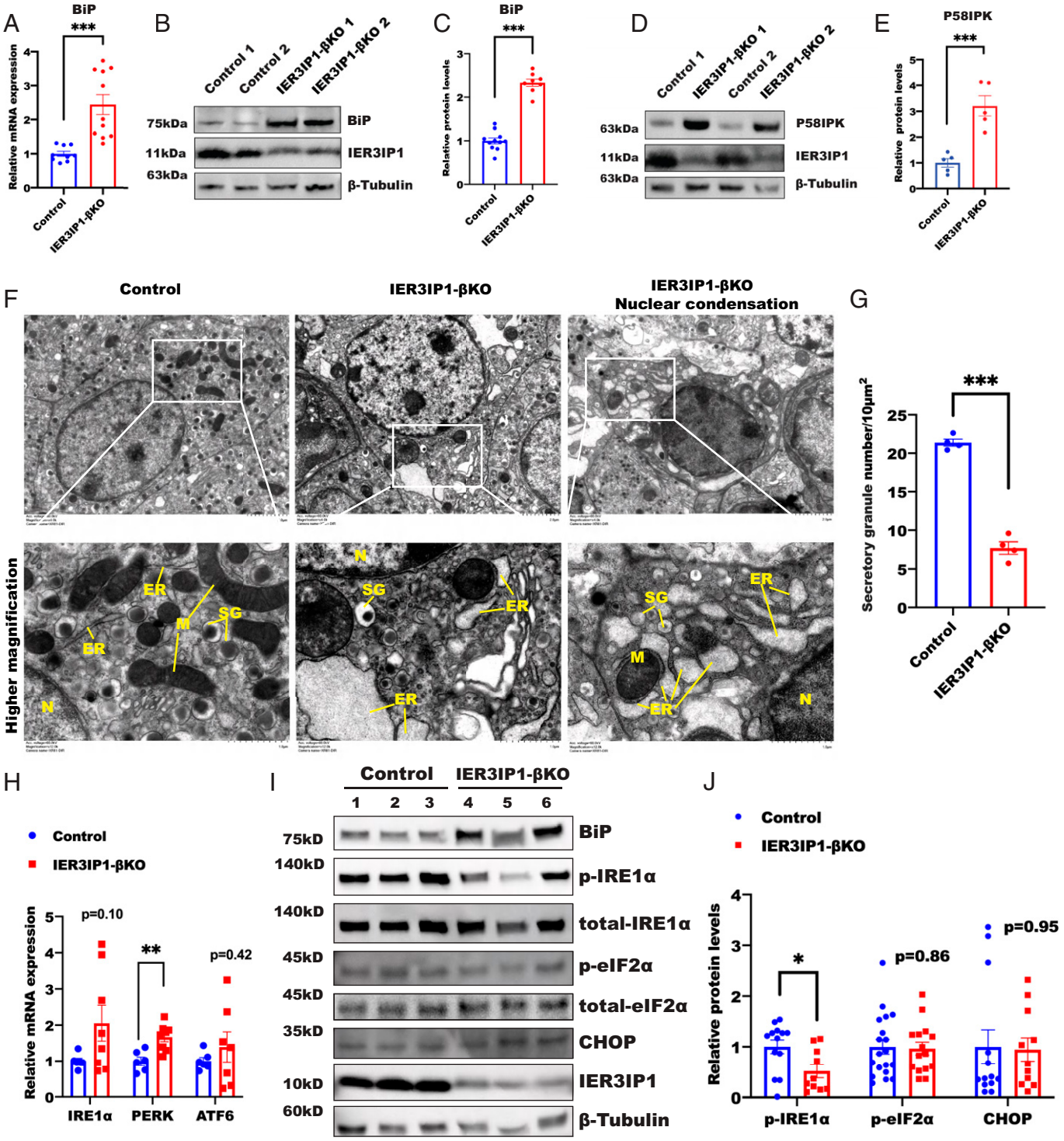

Fig. 3. IER3IP1-βKO induces ER stress without marked activation of UPR. (*A*) mRNA levels of *BiP* from 3-wk-old flox$^{+/+}$ control or IER3IP1-βKO mouse islets (control $n = 9$, βKO $n = 11$). (*B* and *C*) Protein levels of BiP from 3-wk-old flox$^{+/+}$ control or IER3IP1-βKO mouse islets were detected by western blots in *B* and quantified in *C* (control $n = 11$, βKO $n = 8$). (*D* and *E*) Protein levels of P58IPK from 3-wk-old flox$^{+/+}$ control or IER3IP1-βKO mouse islets were detected by western blots in *D* and quantified in *E* ($n = 5$ in each group). (*F*) Representative transmission electron microscopy showing markedly dilated ER in β cells of 3-wk-old IER3IP1-βKO mice, SG: secretory granule, M: mitochondria, N: nuclear. (*G*) Quantification of secretory granules of control or IER3IP1-βKO mouse islets ($n = 4$ in each group, seven random fields per mouse were analyzed). (*H*) mRNA levels of *IRE1α*, *PERK*, and *ATF6* from 3-wk-old flox$^{+/+}$ control or IER3IP1-βKO mouse islets (control $n = 6$, βKO $n = 8$). (*I*) Western blot showing the expression of BiP, phosphorylated IRE1α (p-IRE1α), total-IRE1, phosphorylated eIF2α (p-eIF2α), total-eIF2α, CHOP, and IER3IP1 from 3-wk-old flox$^{+/+}$ control or IER3IP1-βKO mouse islets. (*J*) Protein levels of *I* were quantified in *J* (p-IRE1α control $n = 13$, βKO $n = 10$; p-eIF2α control $n = 19$, βKO $n = 15$; CHOP control $n = 13$, βKO $n = 11$). Values are shown as mean ± SEM. *$P < 0.05$, **$P < 0.01$, and ***$P < 0.001$.

(16.7 mM) glucose for 5 h, we found that, although the absolute amount of proinsulin and insulin was dramatically decreased, the fold increase of proinsulin level in response to high glucose was preserved in IER3IP1-βKO islets (Fig. 2 *D* and *E*). Additionally, the absolute amount of secreted insulin in basal and glucose-stimulated conditions was dramatically decreased (Fig. 2*F*) in proportion to the diminished insulin content (Fig. 2*G*). However, there was no detectable impairment of glucose-stimulated insulin secretion (GSIS) (percentage of secreted insulin in total islet insulin content) in IER3IP1-βKO islets (Fig. 2*H*).

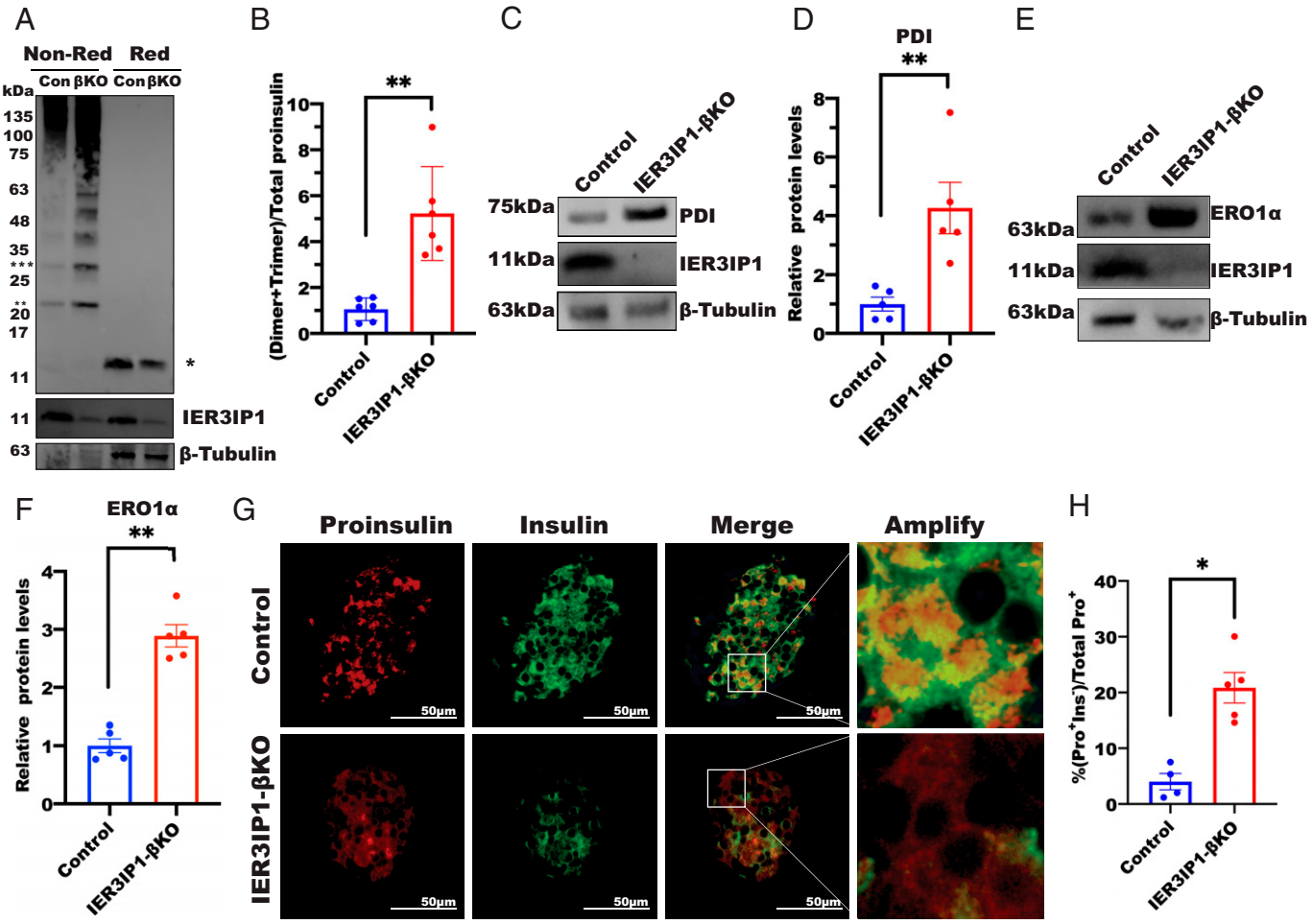

Fig. 4. IER3IP1-βKO impairs oxidative folding of proinsulin in the ER and upregulates the expression of ERO1 and PDI. (*A*) Oxidative folding of proinsulin in islets of 3-wk-old flox$^{+/+}$ control or IER3IP1-βKO mice was analyzed by western blots using antiproinsulin under both nonreducing and reducing conditions. Single asterisk indicated total proinsulin under reducing conditions, double asterisks indicated disulfide-linked proinsulin dimers, and triple asterisks indicated disulfide-linked proinsulin trimers. (*B*) The ratios of proinsulin dimers plus trimers under nonreducing conditions to total proinsulin under reducing conditions were calculated ($n = 6$ in each group). (*C* and *D*) Protein levels of PDI in 3-wk-old flox$^{+/+}$ control and IER3IP1-βKO islets were examined by western blots using anti-PDI in *C* and quantified in *D* ($n = 5$ in each group). (*E* and *F*) Protein levels of ERO1α in 3-wk-old flox$^{+/+}$ control and IER3IP1-βKO islets were examined by western blots using anti-ERO1α in *E* and quantified in *F* ($n = 5$ in each group). (*G*) Representative immunofluorescence images showing staining of anti-insulin (green) and antiproinsulin (red) from 3-wk-old control and IER3IP1-βKO mice. (*H*) Ratio of proinsulin-positive/insulin-negative (Pro$^+$Ins$^-$) cells to total proinsulin positive (Pro$^+$) cells in 3-wk-old flox$^{+/+}$ control and IER3IP1-βKO islets was calculated (control $n = 4$, βKO $n = 5$). Values were shown as mean ± SEM. *$P < 0.05$ and **$P < 0.01$.

These results suggest that decreased insulin secretion in the IER3IP1-βKO mice could be attributed entirely to diminished insulin content rather than an exocytosis defect.

IER3IP1-βKO Induces ER Stress and Impairs Oxidative Folding of Proinsulin in the ER. To examine the role of IER3IP1 in ER homeostasis, we first examined the expression of BiP (a master molecular chaperone regulating the ER function and UPR (27, 28)) and P58IPK (an ER stress marker function as a cochaperone with BiP (29)). We found that both mRNA and protein levels of BiP were increased along with an increase of the protein level of P58IPK in IER3IP1-βKO islets (Fig. 3 *A*–*E*), suggesting that deficiency of IER3IP1 induces ER stress. Consistent with this idea, electron microscopy showed markedly dilated ER along with decreased insulin secretory granules in IER3IP1-βKO islets (Fig. 3 *F* and *G*). Next, we examined the extent of activation of UPR. We found that, although there were trends of increased mRNA expression of IRE1α, PERK, and ATF6, phospho-IRE1 protein (p-IRE1α) and phospho-eIF2α (p-eIF2α), as well as the CHOP protein, were not increased (Fig. 3 *H*–*J*). To determine whether these results are limited by the timing of analysis, we examined the expression of BiP, p58IPK, and genes involved in UPR in 14- to 16-wk-old IER3IP1-βKO mice with very severe diabetes (Fig. 1 *J* and *K*). Again, we found that, although BiP and p58IPK were significantly increased, only PERK was moderately elevated, whereas IRE1 and ATF6 were not increased, even in IER3IP1-βKO mice with severe diabetes (*SI Appendix*, Fig. S5). These results established that IER3IP1 is important for maintaining normal function of the ER, and its deficiency induces ER stress without marked activation of UPR in β cells in vivo.

Proinsulin is the most abundantly synthesized protein in the ER of β cells. Previous studies have shown that proinsulin is predisposed to misfolding, especially upon perturbation of the ER folding environment (16, 30–32). We therefore examined proinsulin oxidative folding under nonreducing conditions (11, 16). We found that, although the total amount of proinsulin was lower in IER3IP1-βKO islets as measured under reducing conditions (Fig. 4 *A*, lane 4 vs. 3), intermolecular disulfide-linked complexes of proinsulin (dimers, trimers, and high-molecular-weight proinsulin–associated complexes) were markedly increased in IER3IP1-βKO islets analyzed under nonreducing conditions (Fig. 4 *A*, lane 2 vs. 1 and quantified in

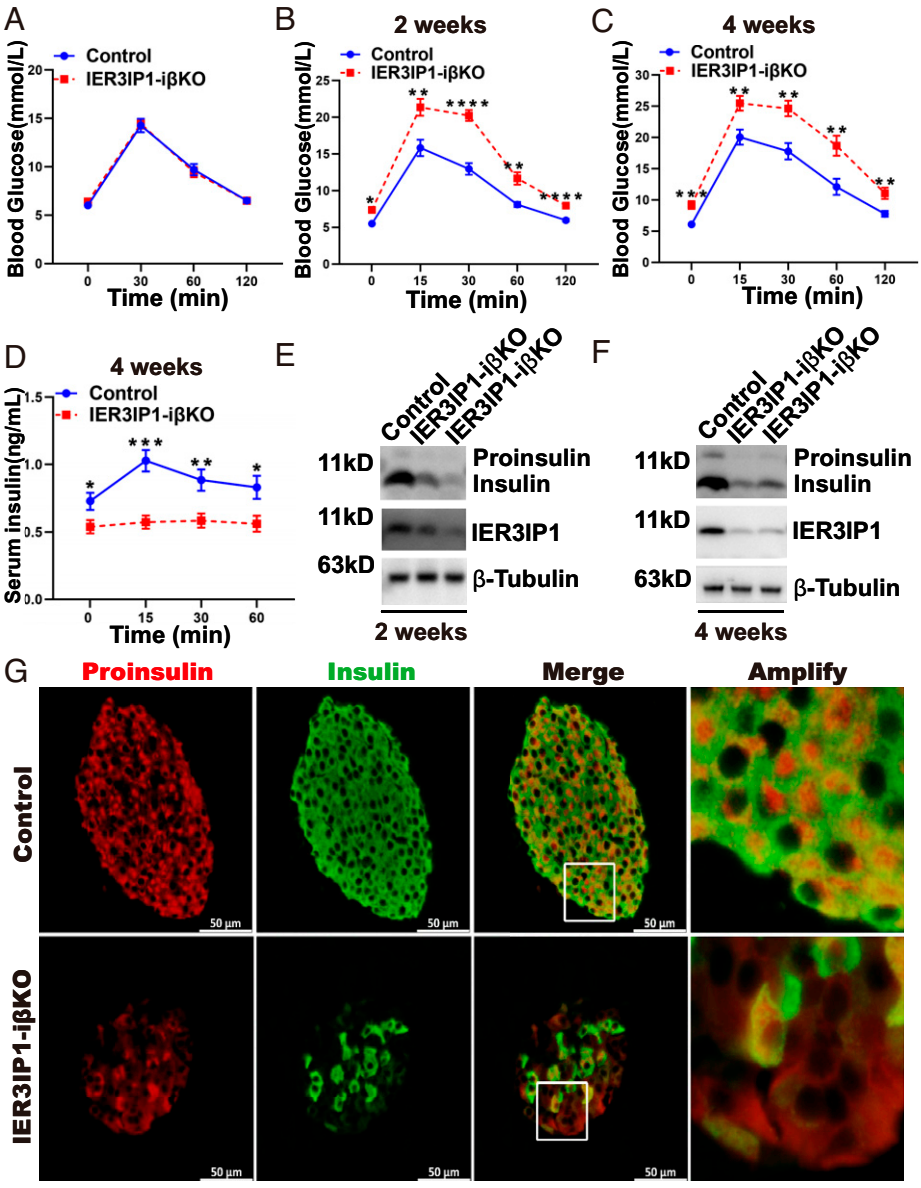

Fig. 5. Inducible deficiency of IER3IP1 in β cells after 8 wk of age decreases insulin content and causes diabetes. The mice of IER3IP1 flox$^{+/+}$ with MIP-CreERT and IER3IP1 flox$^{+/+}$ control were administrated with tamoxifen by intraperitoneal injection at 8 wk old as described in *Methods*. (*A*) Intraperitoneal glucose tolerance tests (IPGTTs) were performed before the injection of tamoxifen (n = 9 in each group). (*B* and *C*) IPGTTs were performed after 2 wk of the tamoxifen injection (*B*) and 4 wk of the injection (*C*) (n = 9 in each group). (*D*) Serum insulin levels of IER3IP1-iβKO and flox$^{+/+}$ control male mice after 4 wk of tamoxifen treatment (n = 9 each group). (*E* and *F*) Protein levels of IER3IP1, proinsulin, and insulin were detected by western blots using freshly isolated islets after 2 wk (*E*) or 4 wk of tamoxifen injection (*F*). (*G*) Representative immunofluorescence images showing staining of anti-insulin (green) and antiproinsulin (red) from IER3IP1-iβKO and flox$^{+/+}$ control male mice after 4 wk of tamoxifen treatment. Values are shown as mean ± SEM. *P < 0.05, **P < 0.01, ***P < 0.001, and ****P < 0.0001.

Fig. 4*B*). Thus, deficiency of IER3IP1 impairs proinsulin oxidative folding in the ER. Consistent with the foregoing observations, PDI and ERO1α, two ER enzymes that affect proinsulin oxidative folding, were both significantly upregulated (Fig. 4 *C*–*F*). Misfolded proinsulin is recognized by ER quality control machinery, preventing its export from the ER to the Golgi complex (14, 16). We therefore examined localization of proinsulin and found that, consistent with our previous findings (14, 33), proinsulin in wild-type β cells was mostly concentrated in the juxtanuclear region (suggesting successful proinsulin trafficking from the ER to the Golgi complex), whereas in IER3IP1-βKO β cells, proinsulin was more diffusely distributed throughout the cytoplasm (additionally, some proinsulin-positive cells lost detectable insulin, i.e., $Pro^{+}Ins^{-}$), suggesting defective anterograde trafficking of proinsulin (Fig. 4 *G* and *H*). These data suggest that defective proinsulin maturation and export from the ER (with impaired insulin production), accompanied by ER stress, exist in β cells with IER3IP1 deficiency.

Inducible IER3IP1 Deficiency in Adulthood Decreases Insulin Content and Causes Diabetes. It is generally accepted that β-cell mass is determined by differentiation and proliferation mostly during embryonic phase and postnatal period, although the balance of proliferation and apoptosis plays a role in maintaining stable β-cell mass throughout life (34, 35). To determine the role of IER3IP1 in β cells after the stage of early development, we deleted IER3IP1 in β cells through tamoxifen-induced Cre recombinase activity in MIP-CreERT-floxed/floxed mice (IER3IP1-iβKO) after 8 wk of age (early adulthood (36)). As shown in Fig. 5 *A* and *B*, both fasting and postload blood glucose were elevated starting from 2 wk after tamoxifen administration, and the hyperglycemia associated with decreased serum insulin was persistent at 4 wk

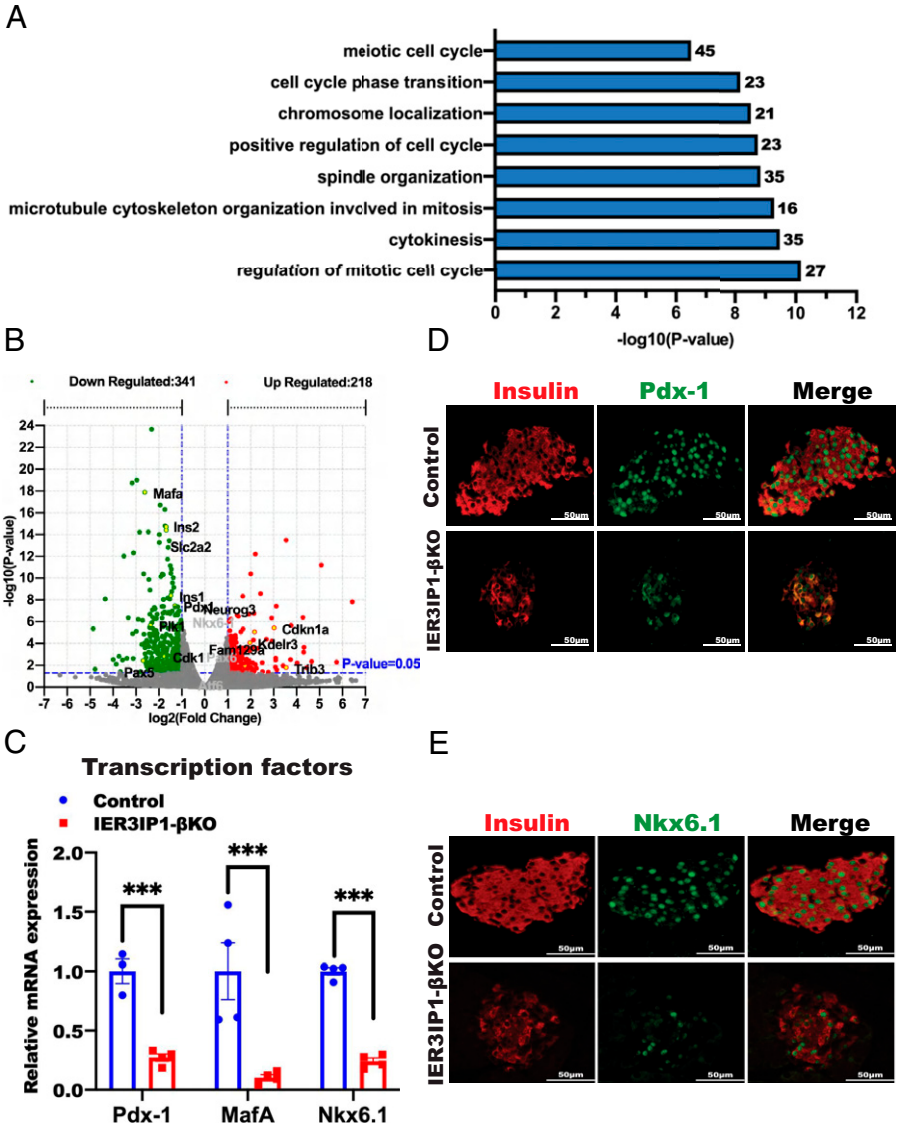

Fig. 6. IER3IP1 deficiency alters the islet transcriptome, affecting cell cycle as well as β-cell identity and maturation. (*A*) GO analyses of RNA-seq data showed significant changes of pathways in the islets from 3-wk-old flox$^{+/+}$ control and IER3IP1-βKO mouse islets. (*B*) Volcano plot depicting transcriptomics data with dotted line marking $P = 0.05$ on *y* axis and fold change of greater than 1 on *x* axis. (*C*) mRNA levels of indicated transcription factors were measured by qRT-PCR in islets of 3-wk-old flox$^{+/+}$ control and IER3IP1-βKO mouse islets (control n = 3–4, βKO n = 4). Values were shown as mean ± SEM. ***$P < 0.001$. (*D* and *E*) Representative immunofluorescence images showing expression nuclear localization of β-cell maturation markers of Pdx-1 (*D*) and Nkx6.1 (*E*) from 3-wk-old flox$^{+/+}$ control and IER3IP1-βKO mice.

after tamoxifen administration (Fig. 5 *C* and *D*). IER3IP1 deficiency in IER3IP1-iβKO mice 2 and 4 wk after giving tamoxifen was confirmed by both immunofluorescence (*SI Appendix*, Fig. S6) and western blotting, which also showed a decrease of proinsulin and insulin content (Fig. 5 *E* and *F*). In addition, immunofluorescence revealed that (consistent with the observation in IER3IP1-βKO islets) (Fig. 4*G*), inducible deficiency of IER3IP1 in adulthood also caused a more-diffuse cytoplasmic distribution of proinsulin and increased Pro^{+}/Ins^{-} cells (Fig. 5*G*). These data demonstrate that IER3IP1 plays an important role in maintaining β-cell function, even after the neonatal period.

IER3IP1 Deficiency Alters the Islet Transcriptome, Affecting Cell Cycle as Well as β-Cell Identity and Maturation. To determine cellular responses triggered by IER3IP1 deficiency, we performed transcriptome analysis using isolated islets from 3-wk-old IER3IP1-βKO and control mice. GO analysis identified significant downregulation of biological pathways associated with cell proliferation (Fig. 6*A*). Using a Log2 fold change and false discovery rate of <0.05, we found that there were 341 downregulated and 218 upregulated genes in IER3IP1-βKO islets compared with that of controls (Fig. 6*B*). The mRNA levels of markedly decreased genes were strongly enriched in key transcription factors known to regulate β-cell maturation and identity, including Mafa, Pdx-1, and Nkx6.1, and these were confirmed by real-time PCR (Fig. 6*C*). We also found that PDX-1 and Mafa were decreased in IER3IP1-βKO mice as early as 2 wk of age (*SI Appendix*, Fig. S7), when blood glucose levels are only mildly elevated (Fig. 1*F*), suggesting that changes in expression of key transcription factors caused by IER3IP1 deficiency occur before the development of overt diabetes. Immunofluorescence staining further validated significant decreases of PDX-1 and NKX6.1 protein in IER3IP1-βKO islets (Fig. 6 *D* and *E*). Similar changes of mRNA levels, and immunostaining of these transcription factors, were observed in IER3IP1-iβKO islets after 2 and 4 wk of tamoxifen injection (*SI Appendix*, Fig. S8). To determine the consequence of downregulation of these key transcription factors, we performed costaining with anti-insulin, antiglucagon, and antisomatostatin. As shown in Fig. 7*A* and quantified in Fig. 7*B*, there was an increase in the abundance and intraislet localization of glucagon-positive, as well as somatostatin-positive, cells in IER3IP1-βKO islets, which accompanied the decrease of insulin-positive cells. Furthermore, there was detection of insulin/glucagon double-positive cells and insulin/somatostatin double-positive cells in the islets of IER3IP1-βKO mice

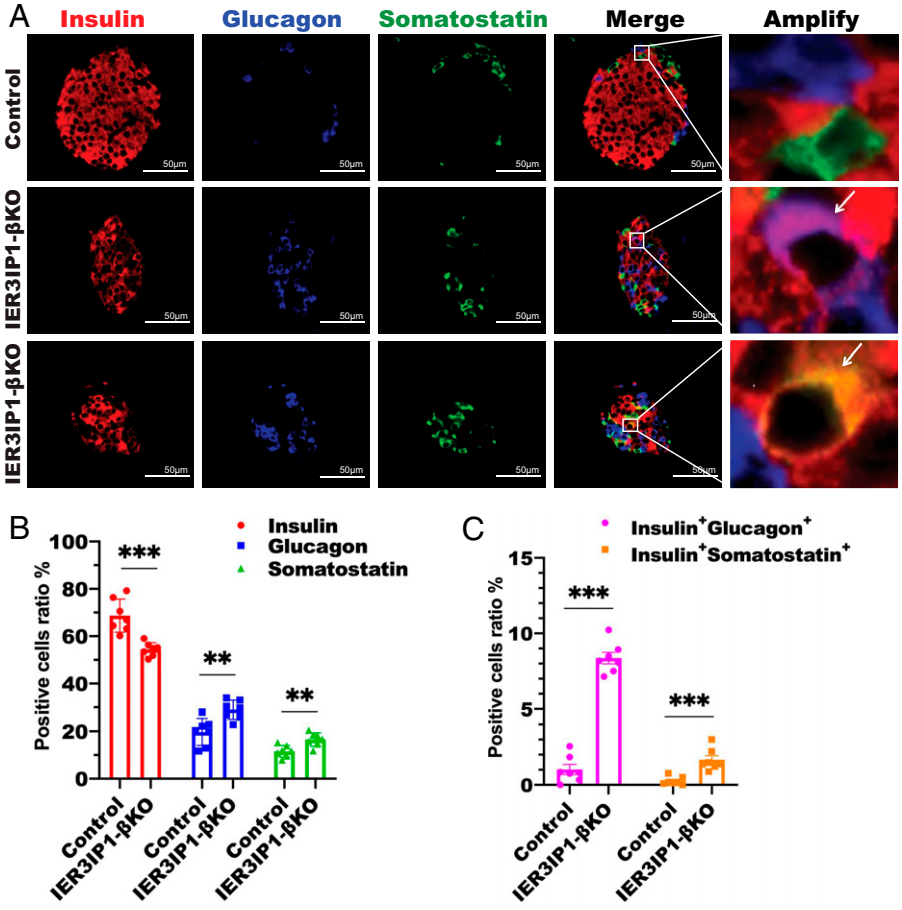

Fig. 7. IER3IP1-βKO decreases insulin-positive cells, increases glucagon- and somatostatin-positive cells, and doubles hormone-positive cells. (*A*) Representative immunofluorescence images showing major islet hormones, anti-insulin (red), antiglucagon (blue), and antisomatostatin (green) in pancreatic sections from 3-wk-old flox$^{+/+}$ control and IER3IP1-βKO mice. (*B*) Percentages of insulin-positive cells, glucagon-positive cells, and somatostatin-positive cells (n = 7 in each group, four sections per pancreas and 4–10 islets per section were analyzed). (*C*) Percentages of insulin and glucagon double-positive cells (Insulin^{+}Glucagon^{+}) and insulin and somatostatin double-positive cells (Insulin^{+}Somatostatin^{+}) (n = 7). Values were shown as mean ± SEM. $^{**}P < 0.01$ and $^{***}P < 0.001$.

(Fig. 7*A* and quantified in Fig. 7*C*). These data demonstrate that β-cell IER3IP1 deficiency results in alterations of transcriptional regulation, leading to impaired β-cell maturation and identity in IER3IP1-βKO mice.

IER3IP1-βKO Causes Decreased Islet Size and β-Cell Mass. Based on the transcriptome changes in Fig. 6, we considered whether IER3IP1 deficiency affects β-cell fate. First, we found that Cdk1 (a core protein of the cell cycle (37)) was significantly downregulated in IER3IP1-βKO islets (Fig. 8*A*), whereas cell growth inhibitors p21/Cdkn1a and p16/Cdkn2a were upregulated (Fig. 8*B*). Second, immunostaining for Ki67 (a nuclear replication marker) showed a significant decrease in 3-wk-old IER3IP1-βKO islets (Fig. 8 *C* and *D*), suggesting diminished β-cell proliferation in the mutant mice. Further, we observed that Trib3 (a mediator of ER stress–induced cell death (38)) was upregulated in IER3IP1-βKO islets (Fig. 8*E*), whereas antiapoptosis regulators, Bcl-2, Bcl-xL, and Mcl-1, were all suppressed (Fig. 8*F*). Similar transcriptional changes of genes involved in cell cycle and apoptosis were observed in IER3IP1-iβKO islets after 4 wk of tamoxifen injection (*SI Appendix*, Fig. S9). Additionally, we noted an increase of nuclear chromatin condensation (39) in IER3IP1-βKO islets by transmission electron microscopy (Fig. 8 *G* and *H*). Taken together, these data suggest that, in conjunction with decreased β-cell proliferation (Fig. 8 *C* and *D*), IER3IP1 deficiency favors β-cell death, contributing to a reduction of mean islet size (Fig. 8 *I* and *J*) and β-cell mass (Fig. 8 *K* and *L*), accounting for the insulin-deficient diabetes in IER3IP1-βKO mice.

Discussion

Although the first case of MEDS caused by homozygous mutations of IER3IP1 was reported more than 10 y ago (20), surprisingly, the function of IER3IP1 and the pathways that it regulates still remain largely unknown. IER3IP1 is an evolutionally conserved protein highly expressed in brain cortex and pancreas (20). Here, we find that IER3IP1 is highly expressed in pancreatic β cells both in human and rodent. Mice lacking IER3IP1 in β cells develop severe, insulin-deficient, early-onset diabetes due to markedly decreased islet size and β-cell mass, accompanied by diminished islet insulin content. Functional studies reveal that β-cell IER3IP1 deficiency induces ER stress and impairs proinsulin oxidative folding in the ER, suggesting that IER3IP1 plays an important role in ER function. Further, IER3IP1-βKO inhibits expression of genes associated with β-cell development, maturation, and survival, which combine to result in a significant reduction of insulin-producing cells that is responsible for the development of severe insulin-deficient diabetes. More importantly, we find that the expression of IER3IP1 is significantly decreased in β cells of patients with T2D, suggesting that deficiency of IER3IP1 may play an important role in β-cell dysfunction in the more-common form of diabetes.

MEDS is a very rare, severe genetic syndrome. All reported patients with MEDS died before 8 y of age (21). Two of the most-severe phenotypes in patients with MEDS are neurological defects, including microcephaly and infantile epileptic encephalopathy, which are likely caused by defects in brain development and integrity, as well as increased apoptosis of neurons (20, 25). Although a recent study shows that IER3IP1

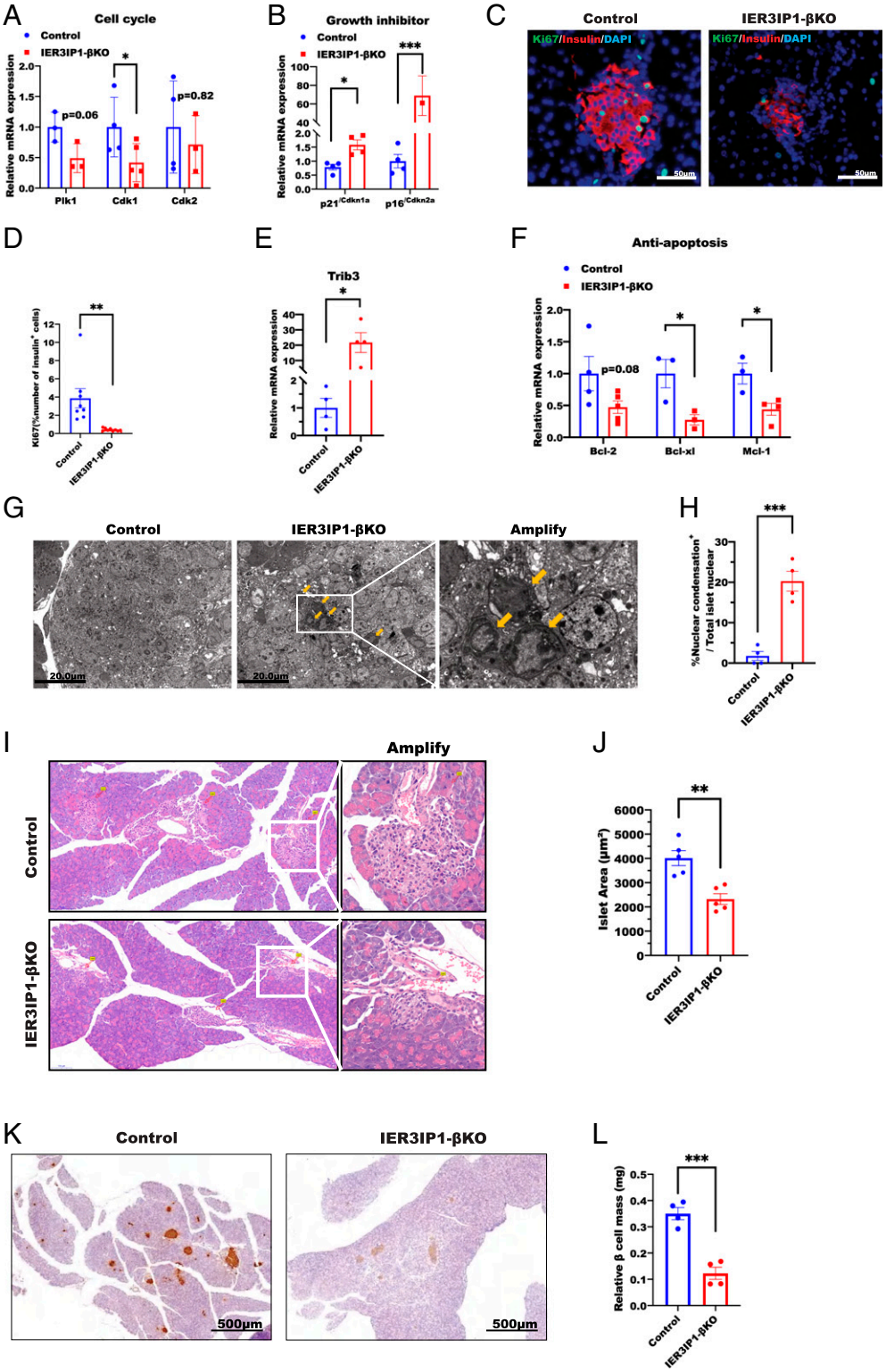

Fig. 8. IER3IP1-βKO causes a reduction of β-cell proliferation and increases abnormal nuclear chromatin condensation. (*A* and *B*) mRNA levels of genes associated with cell cycle in *A* and genes associated with inhibition of cell growth in *B* were examined by qRT-PCR from 3-wk-old flox$^{+/+}$ control and IER3IP1-βKO islets (control n = 3–4, βKO n = 3–5). (*C* and *D*) Representative immunofluorescence images showing the staining of proliferation marker Ki67 from 3-wk-old flox$^{+/+}$ control and IER3IP1-βKO islets were shown in *C*, and percentages of Ki67-positive cells in islet β cells were shown in *D* (n = 8–9 per group, four sections per pancreas and five to eight islets per section were analyzed). (*E*) mRNA levels of Trib3 in 3-wk-old mice of flox$^{+/+}$ control and IER3IP1-βKO islets (n = 4 in each group). (*F*) mRNA levels of antiapoptotic genes in 3-wk-old flox$^{+/+}$ control and IER3IP1-βKO islets (control n = 3–4, βKO n = 3–4). (*G*) Representative electron microscopy images showing chromatin condensation in islets of 3-wk-old IER3IP1-βKO mice. Yellow arrows point to abnormal nucleus. Scale bars: 20.0 μm. (*H*) Quantification of percentages of nuclear condensation in islets of *G*. Cells showing decreased cell diameter, increased density of cytoplasm, as well as pyknosis (condensed chromatin (39)) were quantified in islets of IER3IP1-βKO and control mice (n = 4, at least 40 cells/islet were counted in each mouse). (*I*) Representative hematoxylin and eosin images of pancreatic sections of 3-wk-old control and IER3IP1-βKO mice. (*J*) Quantification of islet area in *I* (n = 5 in each group); eight sections per pancreas and 6–26 islets per section were analyzed. (*K*) Representative images of immunohistochemistry staining of insulin of pancreatic sections of 3-wk-old control and IER3IP1-βKO mice. (*L*) Quantification of islet β-cell mass in *K* (n = 4 in each group); eight sections per pancreas and 6–27 islets per section were analyzed. Values were shown as mean ± SEM. *P < 0.05, **P < 0.01, and ***P < 0.001.

affects neuron survival by regulating ER function and extracellular matrix protein secretion (25), the molecular mechanism underlying the neurological defects remains to be further determined. Another manifestation of MEDS is neonatal diabetes associated with a marked decrease of insulin-positive cells in pancreas (20). In this report, immunostaining demonstrated that IER3IP1 is mainly expressed in pancreatic β cells, but not in α cells and δ cells, in both human and mouse pancreas (Fig. 1 *A* and *B*). Unlike *Ins1*, *Ins2* genes (and some other genes involved in insulin biosynthesis) that are upregulated upon high glucose stimulation, the expression of IER3IP1 was not upregulated in pancreatic islets treated with high glucose (*SI Appendix*, Fig. S2 *B–D*), suggesting that IER3IP1 may not participate directly in insulin biosynthesis.

One of the most-significant changes we observed in IER3IP1-βKO mice was a dramatic decrease in overall islet size and the No. of insulin-producing cells (Figs. 2 and 8 *I–L*). This finding is consistent with autopsy data from the patients with MEDS, showing significant reduction of positive insulin-staining cells (20). Our transcriptomic evidence, and the studies of others, suggest that IER3IP1 may execute its function(s) through three possible interconnected pathways linked to cell proliferation and/or survival. First, IER3IP1 is able to regulate intracellular trafficking and secretion of some proteins crucial for cell development and tissue integrity (25), even in organisms as simple as yeast (24). In this regard, the pathway leading to insulin biosynthesis and storage seemed to be severely affected (Fig. 2 *B* and *C*). However, the fold stimulation of GSIS was not impaired in IER3IP1-βKO islets (Fig. 2 *F–H*), suggesting that IER3IP1 may not directly affect exocytosis of insulin granules. The simplest hypothesis is that IER3IP1 may affect proinsulin ER-to-Golgi transport, which needs to be further explored. Second, IER3IP1 appears to function in the regulation of β-cell fate. Indeed, in IER3IP1-βKO islets, we found that multiple genes associated with cell cycle, proliferation, and maturation were downregulated, whereas genes associated with cell death were upregulated (Figs. 6–8, and *SI Appendix*, Figs. S5, S7, and S8). Additionally, we directly observed diminished β-cell replication and abnormal nuclear chromatin condensation in IER3IP1-βKO islets (Fig. 8 *C*, *D*, *G*, and *H*). Third, it has been reported that IER3IP1 may be involved in homeostatic regulation of the UPR in Min6 cells (26). In support of this general possibility, we found that IER3IP1-βKO causes an upregulation of the ER chaperone BiP and cochaperone P58IPK (Fig. 3 *A–E*) and significant dilation of the ER (Fig. 3*F*), suggesting that IER3IP1 deficiency in β cells leads to ER stress. Nevertheless, phospho-IRE1α and phospho-eIF2α were not increased in the presence of the ER stress in the early stages of diabetes (age of 3 wk, Fig. 3 *H–J*) and sustained hyperglycemia (age of 14–16 wk, *SI Appendix*, Fig. S5), suggesting that IER3IP1 deficiency may dissociate ER stress from UPR activation. Further studies are needed to better understand how IER3IP1 deficiency affects UPR.

Proinsulin is the most-abundant protein in the ER of β cells, accounting for about 10% of total protein synthesis under basal conditions and even more under high glucose stimulation (40). Accumulated genetic and biological evidence indicates that proinsulin is predisposed to misfolding, and an unfavorable ER folding environment can cause increased proinsulin misfolding that may contribute to the development and progression of diabetes (16, 31, 32). In IER3IP1-βKO islets, we do observe an increase of misfolded proinsulin disulfide-linked complexes (Fig. 4*A*), suggesting that IER3IP1 deficiency impairs proinsulin oxidative folding secondary to dysfunction of the ER in IER3IP1-βKO islets. Interestingly, proinsulin misfolding caused by primary defects in proinsulin (due to insulin gene mutations) can also lead to monogenic diabetes (named MIDY [mutant *INS* gene-induced diabetes of youth]) (8). However, unlike MEDS with severe permanent neonatal diabetes, the severity of diabetes phenotypes of patients with MIDY range from neonatal-onset, severe diabetes to mild, late-onset diabetes (6, 10, 41). Although other genetic and environmental factors may contribute, the severity of mutant proinsulin misfolding and its ability to attack coexpressed bystander proinsulin are some of the most important factors driving insulin-deficient diabetes (11, 42, 43). Among all *INS* mutations, proinsulin-C96Y (also called *Akita* proinsulin) that causes early-onset diabetes both in human (44) and mouse (45) is the most studied. Akita male mice develop frank diabetes around 4–8 wk, which is slightly later than that in IER3IP1-βKO mice. Although both IER3IP1-βKO and Akita proinsulin induce ER stress and β-cell death (46), the onset of frank diabetes in IER3IP1-βKO mice appears to be parallel with decreased β-cell mass; nevertheless, markedly elevated blood glucose and insulin deficiency are the earlier events before significantly decreased β-cell mass in Akita mice (47), supporting that primary folding defect of Akita proinsulin that causes decreased insulin production is a primary basis of β-cell failure in Akita mice (13).

In summary, IER3IP1 deficiency in β cells causes dysfunction of the ER with proinsulin misfolding, inducing ER stress with little observable UPR activation, and favoring transcriptomic changes that inhibit β-cell maturation and proliferation along with abnormal nuclear condensation. These features together contribute to markedly decreased β-cell insulin content and diminished β-cell mass, which causes insulin-deficient diabetes that can be observed either in early development (IER3IP1-βKO) or in adulthood (IER3IP1-iβKO). Further studies are warranted to further elucidate how IER3IP1 regulates these pathways that are central to determination of the function and fate of β cells and whether IER3IP1 deficiency contributes to β-cell dysfunction during the development and progression of T2D.

Data, Materials, and Software Availability. All data are included in the manuscript and/or *SI Appendix*.

ACKNOWLEDGMENTS. This work was supported by the National Natural Science Foundation of China (81830025, 81620108004, 81870533, 81900720, 81800733, 82100865, 82070805, and 81870535); we acknowledge the support of the National Key R&D Program of China 2019YFA0802502 and 2020YFA0803704, Tianjin Municipal Science and Technology Bureau (18JCYBJC93900), Tianjin Municipal Human Resources and Social Security Bureau (XB202011 to S.W.), Tianjin Key Medical Discipline (Specialty) Construction Project (TJYXZDXK-030A), and Tianjin Medical University General Hospital Clinical Research Program (22ZYYLCZD02). P.A. was supported by NIH R01 DK048280.

Author affiliations: [a]Department of Endocrinology and Metabolism, Tianjin Medical University General Hospital, Tianjin 300052, China; [b]Department of Endocrinology, The Second Hospital of Tianjin Medical University, Tianjin 300211, China; [c]Organ Transplant Center, Tianjin First Central Hospital, Nankai University, Tianjin 300192, China; [d]NHC Key Laboratory for Critical Care Medicine, Tianjin First Central Hospital, Tianjin 300384, China; [e]Human Islet Resource Center, Tianjin First Central Hospital, Tianjin 300384, China; and [f]Division of Metabolism, Endocrinology & Diabetes, University of Michigan Medical School, Ann Arbor, MI 48105

1. M. Sanyoura, L. H. Philipson, R. Naylor, Monogenic diabetes in children and adolescents: Recognition and treatment options. *Curr. Diab. Rep.* **18**, 58 (2018).
2. M. C. Riddle *et al.*, Monogenic diabetes: From genetic insights to population-based precision in care. Reflections from a diabetes care editors' expert forum. *Diabetes Care* **43**, 3117–3128 (2020).
3. E. De Franco, From biology to genes and back again: Gene discovery for monogenic forms of beta-cell dysfunction in diabetes. *J. Mol. Biol.* **432**, 1535–1550 (2020).
4. E. De Franco *et al.*, YIPF5 mutations cause neonatal diabetes and microcephaly through endoplasmic reticulum stress. *J. Clin. Invest.* **130**, 6338–6353 (2020).
5. H. Wang *et al.*, Biological behaviors of mutant proinsulin contribute to the phenotypic spectrum of diabetes associated with insulin gene mutations. *Mol. Cell. Endocrinol.* **518**, 111025 (2020).
6. M. Liu *et al.*, INS-gene mutations: From genetics and beta cell biology to clinical disease. *Mol. Aspects Med.* **42**, 3–18 (2015).
7. Y. Yang, L. Chan, Monogenic diabetes: What it teaches us on the common forms of Type 1 and Type 2 Diabetes. *Endocr. Rev.* **37**, 190–222 (2016).
8. M. Liu *et al.*, Proinsulin misfolding and diabetes: Mutant INS gene-induced diabetes of youth. *Trends Endocrinol. Metab.* **21**, 652–659 (2010).
9. M. Liu *et al.*, Mutant INS-gene induced diabetes of youth: Proinsulin cysteine residues impose dominant-negative inhibition on wild-type proinsulin transport. *PLoS One* **5**, e13333 (2010).
10. J. Støy *et al.*, In celebration of a century with insulin - Update of insulin gene mutations in diabetes. *Mol. Metab.* **52**, 101280 (2021).
11. J. Sun *et al.*, Role of proinsulin self-association in mutant INS gene-induced diabetes of youth. *Diabetes* **69**, 954–964 (2020).
12. M. Liu *et al.*, Impaired cleavage of preproinsulin signal peptide linked to autosomal-dominant diabetes. *Diabetes* **61**, 828–837 (2012).
13. M. Liu, I. Hodish, C. J. Rhodes, P. Arvan, Proinsulin maturation, misfolding, and proteotoxicity. *Proc. Natl. Acad. Sci. U.S.A.* **104**, 15841–15846 (2007).
14. Y. Huang *et al.*, Defective insulin maturation in patients with type 2 diabetes. *Eur. J. Endocrinol.* **185**, 565–576 (2021).
15. S. Liu *et al.*, Misfolded proinsulin impairs processing of precursor of insulin receptor and insulin signaling in β cells. *FASEB J.* **33**, 11338–11348 (2019).
16. A. Arunagiri *et al.*, Proinsulin misfolding is an early event in the progression to type 2 diabetes. *eLife* **8**, e44532 (2019).
17. D. Shi *et al.*, Genetic syndromes with diabetes: A systematic review. *Obes. Rev.* **22**, e13303 (2021).
18. S. A. Shalev *et al.*, Microcephaly, epilepsy, and neonatal diabetes due to compound heterozygous mutations in IER3IP1: Insights into the natural history of a rare disorder. *Pediatr. Diabetes* **15**, 252–256 (2014).
19. G. M. H. Abdel-Salam *et al.*, A homozygous IER3IP1 mutation causes microcephaly with simplified gyral pattern, epilepsy, and permanent neonatal diabetes syndrome (MEDS). *Am. J. Med. Genet. A.* **158A**, 2788–2796 (2012).
20. C. J. Poulton *et al.*, Microcephaly with simplified gyration, epilepsy, and infantile diabetes linked to inappropriate apoptosis of neural progenitors. *Am. J. Hum. Genet.* **89**, 265–276 (2011).
21. K. Rjiba *et al.*, Further report of MEDS syndrome: Clinical and molecular delineation of a new Tunisian case. *Eur. J. Med. Genet.* **64**, 104285 (2021).
22. I. Valenzuela *et al.*, Microcephaly with simplified gyral pattern, epilepsy and permanent neonatal diabetes syndrome (MEDS). A new patient and review of the literature. *Eur. J. Med. Genet.* **60**, 517–520 (2017).
23. W. H. Yiu, J. W. Poon, S. K. Tsui, K. P. Fung, M. M. Waye, Cloning and characterization of a novel endoplasmic reticulum localized G-patch domain protein, IER3IP1. *Gene* **337**, 37–44 (2004).
24. M. Heidtman, C. Z. Chen, R. N. Collins, C. Barlowe, Yos1p is a novel subunit of the Yip1p-Yif1p complex and is required for transport between the endoplasmic reticulum and the Golgi complex. *Mol. Biol. Cell* **16**, 1673–1683 (2005).
25. C. Esk *et al.*, A human tissue screen identifies a regulator of ER secretion as a brain-size determinant. *Science* **370**, 935–941 (2020).
26. J. Sun, D. Ren, IER3IP1 deficiency leads to increased β-cell death and decreased β-cell proliferation. *Oncotarget* **8**, 56768–56779 (2017).
27. K. F. R. Pobre, G. J. Poet, L. M. Hendershot, The endoplasmic reticulum (ER) chaperone BiP is a master regulator of ER functions: Getting by with a little help from ERdj friends. *J. Biol. Chem.* **294**, 2098–2108 (2019).
28. M. C. Kopp, N. Larburu, V. Durairaj, C. J. Adams, M. M. U. Ali, UPR proteins IRE1 and PERK switch BiP from chaperone to ER stress sensor. *Nat. Struct. Mol. Biol.* **26**, 1053–1062 (2019).
29. D. T. Rutkowski *et al.*, The role of p58IPK in protecting the stressed endoplasmic reticulum. *Mol. Biol. Cell* **18**, 3681–3691 (2007).
30. J. Qiao *et al.*, A distinct role of STING in regulating glucose homeostasis through insulin sensitivity and insulin secretion. *Proc. Natl. Acad. Sci. U.S.A.* **119**, e2101848119 (2022).
31. E. Zito, K. T. Chin, J. Blais, H. P. Harding, D. Ron, ERO1-beta, a pancreas-specific disulfide oxidase, promotes insulin biogenesis and glucose homeostasis. *J. Cell Biol.* **188**, 821–832 (2010).
32. M. Liu, Y. Li, D. Cavener, P. Arvan, Proinsulin disulfide maturation and misfolding in the endoplasmic reticulum. *J. Biol. Chem.* **280**, 13209–13212 (2005).
33. L. Haataja *et al.*, Proinsulin intermolecular interactions during secretory trafficking in pancreatic β cells. *J. Biol. Chem.* **288**, 1896–1906 (2013).
34. D. T. Finegood, L. Scaglia, S. Bonner-Weir, Dynamics of beta-cell mass in the growing rat pancreas. Estimation with a simple mathematical model. *Diabetes* **44**, 249–256 (1995).
35. E. Montanya, V. Nacher, M. Biarnés, J. Soler, Linear correlation between beta-cell mass and body weight throughout the lifespan in Lewis rats: Role of beta-cell hyperplasia and hypertrophy. *Diabetes* **49**, 1341–1346 (2000).
36. S. Dutta, P. Sengupta, Men and mice: Relating their ages. *Life Sci.* **152**, 244–248 (2016).
37. D. Santamaría *et al.*, Cdk1 is sufficient to drive the mammalian cell cycle. *Nature* **448**, 811–815 (2007).
38. N. Ohoka, S. Yoshii, T. Hattori, K. Onozaki, H. Hayashi, TRB3, a novel ER stress-inducible gene, is induced via ATF4-CHOP pathway and is involved in cell death. *EMBO J.* **24**, 1243–1255 (2005).
39. M. Leist, M. Jäättelä, Four deaths and a funeral: From caspases to alternative mechanisms. *Nat. Rev. Mol. Cell Biol.* **2**, 589–598 (2001).
40. J. Sun *et al.*, Proinsulin misfolding and endoplasmic reticulum stress during the development and progression of diabetes. *Mol. Aspects Med.* **42**, 105–118 (2015).
41. M. Liu *et al.*, Normal and defective pathways in biogenesis and maintenance of the insulin storage pool. *J. Clin. Invest.* **131**, e142240 (2021).
42. Y. Yang *et al.*, A novel nonsense INS mutation causes inefficient preproinsulin translocation into the endoplasmic reticulum. *Front. Endocrinol. (Lausanne)* **12**, 774634 (2022).
43. L. Haataja *et al.*, Distinct states of proinsulin misfolding in MIDY. *Cell. Mol. Life Sci.* **78**, 6017–6031 (2021).
44. J. Støy *et al.*; Neonatal Diabetes International Collaborative Group, Insulin gene mutations as a cause of permanent neonatal diabetes. *Proc. Natl. Acad. Sci. U.S.A.* **104**, 15040–15044 (2007).
45. J. Wang *et al.*, A mutation in the insulin 2 gene induces diabetes with severe pancreatic β-cell dysfunction in the Mody mouse. *J. Clin. Invest.* **103**, 27–37 (1999).
46. S. Oyadomari *et al.*, Targeted disruption of the Chop gene delays endoplasmic reticulum stress-mediated diabetes. *J. Clin. Invest.* **109**, 525–532 (2002).
47. S. Gupta, B. McGrath, D. R. Cavener, PERK (EIF2AK3) regulates proinsulin trafficking and quality control in the secretory pathway. *Diabetes* **59**, 1937–1947 (2010).